

# Electrochemical Generation of Rhodium Porphyrin Hydrides. Catalysis of Hydrogen Evolution

Valérie Grass, Doris Lexa,<sup>1</sup> and Jean-Michel Savéant\*

Contribution from the Laboratoire d'Electrochimie Moléculaire de l'Université Denis Diderot, Unité Associée au CNRS No 438, 2 place Jussieu, 75251 Paris Cedex 05, France

Received November 27, 1996. Revised Manuscript Received March 12, 1997<sup>⊗</sup>

**Abstract:** In polar solvents, Rh(III) porphyrins are directly reduced in Rh(I) complexes which react readily with Brønsted acids to give Rh(III) hydrides. They then undergo, at a more negative potential, an additional electron uptake to yield the corresponding Rh(II) hydrides. The electrogenerated rhodium(II) complex is the key intermediate of catalytic hydrogen evolution according to a mechanism which heavily depends on the solvent and on axial ligands. In DMSO, hydride transfer from Rh(II)H<sup>-</sup> to the acid, yielding H<sub>2</sub>, competes with hydride transfer reduction of the solvent by both Rh(III)H and Rh(II)H<sup>-</sup>. In a less-complexing solvent, such as butyronitrile, hydrogen evolution occurs both by hydride transfer to the acid and H-atom abstraction to the solvent. The latter pathway is shut off by the addition of strong and soft ligands such as tertiary phosphines. With PEt<sub>3</sub>, a particularly strong electron-donating ligand, not only Rh(II)H<sup>-</sup> but also Rh(III)H triggers H<sub>2</sub> evolution. The various changes of the hydrogen evolution mechanism as well as the stability of the catalyst can be rationalized by the variation of the electron density distribution brought about by the presence or the absence of the axial ligand.

Low-valent or high-valent metalloporphyrins offer a vast range of potentialities for activating inert molecules.<sup>2</sup> Electrochemistry is a particularly convenient tool for generating such nonconventional oxidation states and observing in situ their reactions with the target substrate. Another facet of the same question is that once a metalloporphyrin has proven active toward a particular substrate, it may be used as homogeneous chemical<sup>3</sup> catalyst for the electrochemical oxidation or reduction of this substrate.

<sup>⊗</sup> Abstract published in *Advance ACS Abstracts*, July 1, 1997.

(1) Permanent address: Laboratoire de Bioénergétique et Ingénierie des Protéines, UPR CNRS 9036, 31 Chemin J. Aiguier, 13009 Marseille, France.

(2) (a) Such as, on the reductive side, dioxygen,<sup>2b-h</sup> carbon dioxide,<sup>2i-l</sup> NO, NO<sub>2</sub>, and NO<sub>3</sub><sup>2-</sup>.<sup>2m-s</sup> (b) Collman, J. P.; Marroco, M.; Denisevich, P.; Koval, C.; Anson, F. C. *J. Electroanal. Chem. Interfacial Electrochem.* **1979**, *101*, 117. (c) Chang, C. K.; Liu H. Y.; Abdalmuhdi, I. *J. Am. Chem. Soc.* **1984**, *106*, 2725. (d) Collman, J. P.; Wagenknecht, P. S.; Hutchison, J. E. *Angew. Chem., Int. Ed. Engl.* **1994**, *33*, 1537. (e) Shi, C.; Anson, F. C. *J. Am. Chem. Soc.* **1991**, *113*, 9564. (f) Shi, C.; Anson, F. C. *Inorg. Chem.* **1992**, *31*, 5078. (g) Steiger, B.; Anson, F. C. *Inorg. Chem.* **1995**, *34*, 3355. (h) Shi, C.; Anson, F. C. *Inorg. Chem.* **1995**, *34*, 4554. (i) Hammouche, M.; Lexa, D.; Savéant, J.-M. *J. Am. Chem. Soc.* **1987**, *113*, 8455. (j) Bhugun, I.; Lexa, D.; Savéant, J.-M. *J. Am. Chem. Soc.* **1994**, *116*, 5015. (k) Bhugun, I.; Lexa, D.; Savéant, J.-M. *J. Am. Chem. Soc.* **1996**, *118*, 1769. (l) Bhugun, I.; Lexa, D.; Savéant, J.-M. *J. Phys. Chem.* In press. (m) Choi, I.; Ryan, M. *New J. Chem.* **1992**, *16*, 591. (n) Kyu Choi, I.; Liu, Y.; Feng, D.; Paeng, K.; Ryan, M. *Inorg. Chem.* **1991**, *30*, 1832. (o) Fernandez, J.; Feng, D.; Chang, A.; Keyser, A.; Ryan, M. *Inorg. Chem.* **1986**, *25*, 2606. (p) Feng, D.; Ting, Y.; Ryan, M. *Inorg. Chem.* **1985**, *24*, 612. (q) Choi, I.; Ryan, M. *Chim. Acta* **1988**, *153*, 25. (r) Barley, M.; Takeuchi, K.; Murphy, W.; Meyer, T. *J. Chem. Soc., Chem. Commun.* **1985**, 507. (s) Barley, M.; Takeuchi, K.; Meyer, T. *J. Am. Chem. Soc.* **1986**, *108*, 5876.

(3) (a) Although low-valent metalloporphyrins may be generated by a simple outersphere single electron transfer from the electrode, it is expected that they will not themselves react with the substrate as outersphere electron donors but rather that they will integrate transiently the substrate into their coordination sphere. Such chemical catalytic processes, involving inner-sphere pathways, are indeed expected to be more efficient, both in terms of rate and selectivity, than redox catalytic processes in which catalysis has a physical origin, namely, the electron donor is dispersed three-dimensionally instead of being confined on a surface as in the direct electrochemical reaction.<sup>3b,c</sup> (b) Andrieux, C. P.; Dumas-Bouchiat, J.-M.; Savéant, J.-M. *J. Electroanal. Chem.* **1978**, *87*, 39. (c) Andrieux, C. P.; Savéant, J.-M. *Electrochemical Reactions. In Investigations of Rates and Mechanisms; Bernasconi, C. F., Ed.; Wiley: New York, 1986; Vol. 6, 4/E, Part 2, p 305.*

Hydrides of rhodium porphyrins may be synthesized by chemical means. One method consists in reducing a rhodium(III) porphyrin into the corresponding rhodium(I) complex by sodium borohydride. The latter compound is then protonated by acetic acid.<sup>4</sup> Another possibility is to react a Rh(II)–Rh(II) metal dimer with molecular hydrogen in an apolar solvent such as benzene.<sup>5</sup> So far, hydrides of rhodium(III) porphyrins have been used for inserting small molecules such as carbon monoxide, ketones, and aldehydes into the Rh–H bond.<sup>6</sup> The intermediacy of rhodium(III) porphyrin hydride has also been suggested in the photo-dehydrogenation of isopropanol into acetone.<sup>7</sup>

The easy formation of rhodium(III) porphyrin hydrides from rhodium(I) porphyrin suggests possible applications in homogeneous catalysis of electrochemical reactions such as hydrogen evolution from acids and hydrogenation reactions. One may indeed conceive an electrocatalytic process where the rhodium(III) porphyrin would be reduced into rhodium(I) which would

(4) (a) Hoshino, M.; Yasufu, K.; Seki, H.; Yamasaki, H. *J. Phys. Chem.* **1985**, *89*, 3080. (b) Ogoshi, H.; Setsune, J.; Yoshida, Z. *J. Am. Chem. Soc.* **1977**, *99*, 3869. (c) Setsune, J.; Yoshida, Z.; Ogoshi, H. *J. Chem. Soc., Perkin Trans.* **1982**, 983.

(5) (a) Wayland, B. B.; Ba, S.; Sherry, A. E. *Inorg. Chem.* **1992**, *31*, 148. (b) Bosch, H. W.; Wayland, B. B. *J. Organomet. Chem.* **1986**, 317. (c) Wayland, B. B.; Ba, S.; Sherry, A. E. *J. Am. Chem. Soc.* **1991**, *113*, 5305. (d) Paonessa, R. S.; Nicholas, C. T.; Halpern, J. *J. Am. Chem. Soc.* **1985**, *107*, 4333. (e) Wayland, B. B. *Polyhedron* **1988**, *7*, 1545. (f) Del Rossi, K. J.; Zhang, X.-X.; Wayland, B. B. *J. Organomet. Chem.* **1995**, 47.

(6) (a) Wayland, B. B.; Duttaahmed, A.; Woods, B. A. *J. Chem. Soc., Chem. Commun.* **1983**, 142. (b) Farnos, M. D.; Woods, B. A.; Wayland, B. B. *J. Am. Chem. Soc.* **1986**, *108*, 3659. (c) Wayland, B. B.; Woods, B. A.; Coffin, V. L. *Organometallics* **1986**, *5*, 1059. (d) Wayland, B. B.; Van Voorhees, S. L. *Organometallics* **1987**, *6*, 204. (e) Wayland, B. B.; Sherry, A. E.; Coffin, V. C. *J. Chem. Soc., Chem. Commun.* **1989**, 662. (f) Wayland, B. B.; Sherry, A. E.; Posznick, G.; Bunn, A. G. *J. Am. Chem. Soc.* **1992**, *114*, 1673. (g) Wayland, B. B.; Woods, B. A.; Minda, V. M. *J. Chem. Soc., Chem. Commun.* **1982**, 634. (h) Wayland, B. B.; Woods, B. A.; Pierce, R. *J. Am. Chem. Soc.* **1982**, *104*, 302. (i) Wayland, B. B.; Voorhees, S. L.; Wilker, C. *Inorg. Chem.* **1986**, *25*, 4039. (j) Wayland, B. B.; Woods, B. A. *J. Chem. Soc., Chem. Commun.* **1981**, 700. (k) Wayland, B. B.; Balkus, K. J.; Farnos, M. D. *Organometallics* **1989**, *8*, 950. (l) Del Rossi, K.; Wayland, B. B.; Zhang, X.-X. *J. Organomet. Chem.* **1995**, 504, 47.

(7) (a) Irie, R.; Li, X.; Saito, Y. *J. Mol. Catal.* **1983**, *18*, 263. (b) Irie, R.; Li, X.; Saito, Y. *J. Mol. Catal.* **1984**, *23*, 17.

then be converted into the rhodium(III) hydride by an acid added to the solution. The  $\text{H}^-$  donor properties of this hydride or also those of its reduced form,  $\text{Rh(II)H}^-$ , would be used in hydrogen evolution or hydrogenation reactions. As far as hydrogen evolution from acids is concerned, it has been shown to be catalyzed by low-valent porphyrins of cobalt,<sup>8</sup> ruthenium,<sup>9</sup> and iron.<sup>10</sup>

As shown recently,<sup>11</sup> the electrochemical reduction of rhodium(III) porphyrins in aprotic polar solvents proceeds directly to the rhodium(I) oxidation state. More precisely, the rhodium(II) complex formed after the first electron uptake undergoes a rapid ligand exchange reaction which produces a secondary rhodium(II) complex that is easier to reduce than the starting rhodium(III) porphyrin at the electrode surface (ECE pathway). Concurrently, the two rhodium(II) complexes disproportionate by means of electron transfer from the former to the latter complex yielding the rhodium(I) porphyrin and regenerating the starting rhodium(III) complex (disproportionation pathway).<sup>12</sup> This two-electron process may be converted into two successive one-electron reversible reactions by strong and soft ligands that stabilize the Rh(II) oxidation state (a typical example is triethylphosphine).

As reported below, the rhodium(I) porphyrins thus generated electrochemically may be reacted with Brønsted acids so as to produce in situ the corresponding rhodium(III) hydrides. The latter complexes may then be further reduced in situ, affording the rhodium(II) hydride. The hydride is more reactive toward the acid at the Rh(II) than at the Rh(III) oxidation state thus allowing a more efficient catalysis of hydrogen evolution. Since the manner in which Rh(I) is generated from Rh(III) may be modified by strong and soft ligands, the effect of tertiary phosphines on the formation of the hydride and on catalysis of hydrogen evolution will also be described. All experiments were performed with TPPRhI (TPP 5,10,15,20-tetraphenylporphyrin)

## Results and Discussion

**Hydrides from the Reaction of Rhodium(I) Porphyrins with Brønsted Acids.** Figure 1 shows the effect of the addition of a strong acid,  $\text{HCO}_2\text{H}$ , on the cyclic voltammetry of TPPRhI in DMSO. In the absence of acid, the voltammogram (Figure 1a) exhibits a two-electron quasi-reversible wave corresponding to the ECE–disproportionation conversion of the initial Rh(III) complex into Rh(I). At the second reversible one-electron wave, one additional electron is injected into the Rh(I) complex, presumably in the porphyrin ring.<sup>11</sup> When  $\text{HCO}_2\text{H}$  is added, the first wave becomes irreversible and increases, exhibiting a

(8) (a) Connolly, P.; Espenson, J. H. *Inorg. Chem.* **1986**, *25*, 2684. (b) Kellett, R. M.; Spiro, T. G. *Inorg. Chem.* **1985**, *24*, 2378. (c) Kellett, R. M.; Spiro, T. G. *Inorg. Chem.* **1985**, *24*, 2373.

(9) (a) Collman, J. P.; Ha, Y.; Guillard, R.; Lopez, M.-A. *Inorg. Chem.* **1993**, *32*, 1788. (b) Collman, J. P.; Wagenknecht, P. S.; Hembre, R. T.; Lewis, N. S. *J. Am. Chem. Soc.* **1990**, *112*, 1294. (c) Collman, J. P.; Wagenknecht, P. S.; Hutchison, J. E.; Lewis, N. S.; Guillard, R.; Lopez, M.-A.; L'Her, M.; Bothner-By, A. A.; Mishra, P. K. *J. Am. Chem. Soc.* **1992**, *114*, 5654. (d) Collman, J. P.; Ha, Y.; Guillard, R.; Lopez, M.-A.; Wagenknecht, P. S. *J. Am. Chem. Soc.* **1993**, *115*, 9080. (e) Collman, J. P.; Wagenknecht, P. S.; Hutchison, J. E. *Angew. Chem., Int. Ed. Engl.* **1994**, *33*, 1537. (f) Collman, J. P.; Wagenknecht, P. S.; Hutchison, J. E. *J. Am. Chem. Soc.* **1992**, *114*, 5665.

(10) Bhugun, I.; Lexa, D.; Savéant, J.-M. *J. Am. Chem. Soc.* **1996**, *118*, 3982.

(11) Grass, V.; Momenteau, M.; Lexa, D.; Savéant, J.-M. *J. Am. Chem. Soc.* **1997**, *119*, 3536.

(12) (a) This "ECE-disproportionation" process is responsible for the irreversibility of the rhodium(III) reduction rather than metal–metal dimerization of the initially formed rhodium(II) complex as believed earlier.<sup>12b,c</sup> (b) Kadish, K. M.; Yao, C.-L.; Anderson, J. E.; Cocolios, P. *Inorg. Chem.* **1985**, *24*, 4515. (c) Kadish, K. M.; Hu, Y.; Boschi, T.; Tagliatesta, P. *Inorg. Chem.* **1993**, *32*, 2996.

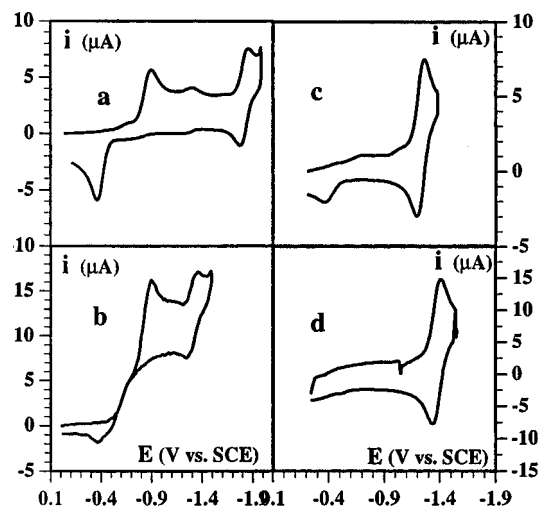


**Figure 1.** Cyclic voltammetry of 1 mM TPPRhI in DMSO + 0.1 M  $\text{Et}_4\text{NClO}_4$  in the absence (a) and in the presence (b) of 50 mM  $\text{HCO}_2\text{H}$ . Parts c and d represent the voltammograms recorded after electrolysis at  $-1.0$  V vs SCE in the presence of 2 mM  $\text{HCO}_2\text{H}$ . Scan rate: 0.1 (a–c), 0.4 (d) V/s.

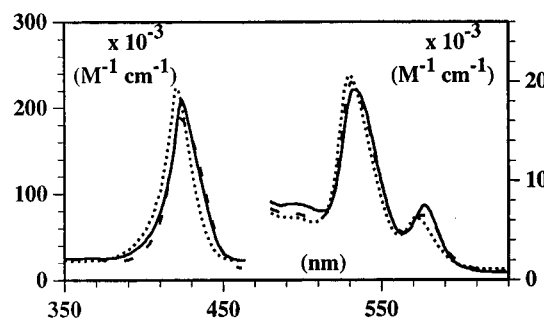


**Figure 2.** Thin-layer spectroelectrochemistry of TPPRhI (0.25 mM) in DMSO + 0.1 M  $\text{Et}_4\text{NClO}_4$  in the presence of 50 mM  $\text{HCO}_2\text{H}$ . Solid line: initial complex. Dotted line: after electrolysis at  $-1.0$  V vs SCE. Dashed line: intermediary spectrum.

catalytic character. These observations will be discussed later. For the moment, we focus attention on the new, almost reversible, wave which appears at a more negative potential. Its potential location is close to that of the reversible wave of  $\sigma$ -alkylrhodium(III) complexes that are produced in situ from the reaction of Rh(I) with alkyl halides. This is a first clue of the formation of a Rh(III)H complex upon reaction of the electrogenerated Rh(I) complex with the acid. The electrochemical properties of this presumed RhH porphyrin are better seen after electrolyzing the solution just beyond the peak of the irreversible two-electron wave where Rh(III) is reduced into Rh(I). The hydride wave is thus the only wave present in the voltammogram. Under these conditions, the reversibility of the Rh(III)H/  $\text{Rh(II)H}^-$  wave clearly appears when the scan rate is raised to 0.4 V/s (Figure 1d), while at a lower scan rate, a partial decomposition of the  $\text{Rh(II)H}^-$  complex is observed (Figure 1c).

A further indication of the formation of the hydride is provided by thin-layer spectroelectrochemistry (Figure 2). The spectrum obtained after electrolysis in the presence of the acid is similar to the spectrum of the Rh(III) methyl complex and is very close to the spectrum recently obtained in a pulse radiolytic study of the reduction of rhodium(III) porphyrins in the presence of an acid in isopropanol.<sup>13</sup> As for Rh(III)R, the spectrum is, as expected, not very different from that of the starting Rh(III) complex.

(13) Grodkowski, J.; Neta, P.; Hambright, P. *J. Phys. Chem.* **1995**, *99*, 6019.

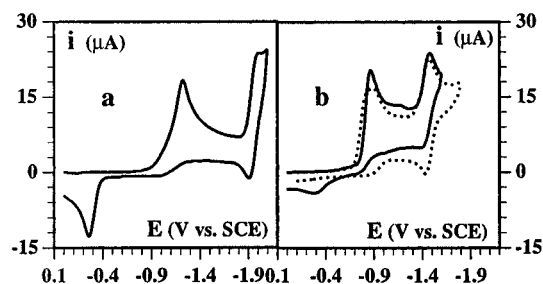
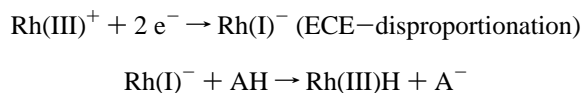


**Figure 3.** Cyclic voltammety of 1 mM TPPRhI in butyronitrile + 0.1 M *n*-Bu<sub>4</sub>NClO<sub>4</sub>: (a) with no acid and no phosphine added; (b) after addition of 2 mM CNCH<sub>2</sub>CO<sub>2</sub>H (full line), after further addition of 0.1 M PPh<sub>3</sub>. Scan rate: 0.1 V/s.

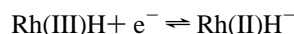
This assignment received further confirmation from IR spectroscopy. The spectrum recorded after electrolysis in the presence of the acid exhibits a band at 2050 cm<sup>-1</sup> in agreement with literature (2095 cm<sup>-1</sup> in Nujol<sup>3c</sup> and 2200 cm<sup>-1</sup> in a KBr pellet;<sup>2b</sup> the bands of the various metal hydrides<sup>14</sup> range from 1800 to 2200 cm<sup>-1</sup>).

The hydride complex is formed in the same way in a less-ligating solvent such as butyronitrile (Figure 3), although the Rh(III)H/Rh(II)H<sup>-</sup> wave is less reversible than that in DMSO (Figure 3b). This improved stability of the Rh(II)H<sup>-</sup> in DMSO is likely to result from axial ligation by a solvent molecule. The stabilizing role of axial ligand is confirmed by the observation that reversibility is significantly enhanced by the addition of a strong ligand, namely triphenylphosphine, to the butyronitrile solution (Figure 3b). The stabilizing effect of the triphenylphosphine ligand is also revealed by thin-layer spectroelectrochemistry which corresponds to longer times than cyclic voltammety (minutes instead of seconds). The spectrum of Rh(III)H could be obtained in the presence of the phosphine but not in its absence. It is then very similar to the one recorded in DMSO.

We may thus conclude that rhodium(III) porphyrin hydrides can be obtained by protonation by strong acids of the rhodium(I) complex generated by the two-electron reduction of the rhodium(III) porphyrin:



The rhodium(III) hydride thus obtained may accept one electron yielding an Rh(II)H<sup>-</sup> complex:



whose stability and fate depends on the solvent and of axial ligation as described in the next section.

**Catalysis of Hydrogen Evolution.** In DMSO, when a stronger acid than formic acid, namely trifluoroacetic acid ( $pK_a = 3.75$  instead of 10.4<sup>15</sup>)<sup>15</sup> is used, the Rh(III)/Rh(I) wave takes a catalytic character (Figure 1b). This is also the case for the Rh(III)H/Rh(II)H<sup>-</sup> wave when more and more acid is added. Two preparative scale electrolyses were carried out in the aim of measuring hydrogen evolution, one at -1 V vs SCE at the level of the Rh(III)/Rh(I) wave and the other at -1.6 V vs SCE at the level of the Rh(III)H/Rh(II)H<sup>-</sup> wave. No hydrogen was

(14) Adams, D. A. In *Metal-Ligand and Related Vibrations*; Edward Arnold, Ltd.: London, 1967; pp 1-25.

(15) (a) From ref 17a for CF<sub>3</sub>CO<sub>2</sub>H and from interpolation between water<sup>15c</sup> and DMSO values for HCO<sub>2</sub>H. (b) Bordwell, F. G. *Acc. Chem. Res.* **1988**, *21*, 456. (c) *Handbook of Chemistry and Physics*, 72th ed.; CRC Press: Boca Raton, FL, 1991; pp 8-39, 40.

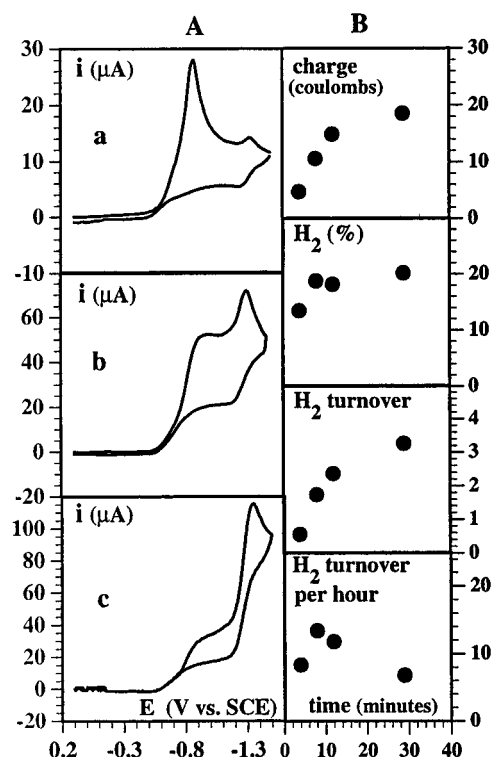
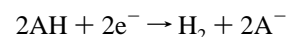


**Figure 4.** (A) Cyclic voltammety of 1 mM TPPRhI in DMSO + 0.1 M Et<sub>4</sub>NClO<sub>4</sub> in the presence of CF<sub>3</sub>CO<sub>2</sub>H (a, 2; b, 10; c, 50 mM). Scan rate: 0.1 V/s. (B) Electrolysis at -1.6 V vs SCE in the presence of 20 mM CF<sub>3</sub>CO<sub>2</sub>H.

detected after the first electrolysis, which rather produced dimethyl sulfide by reduction of DMSO. The same reaction also takes place during the second electrolysis, but this time, hydrogen was simultaneously produced with a faradaic yield of the order of 20% as determined on the basis of the following stoichiometry:

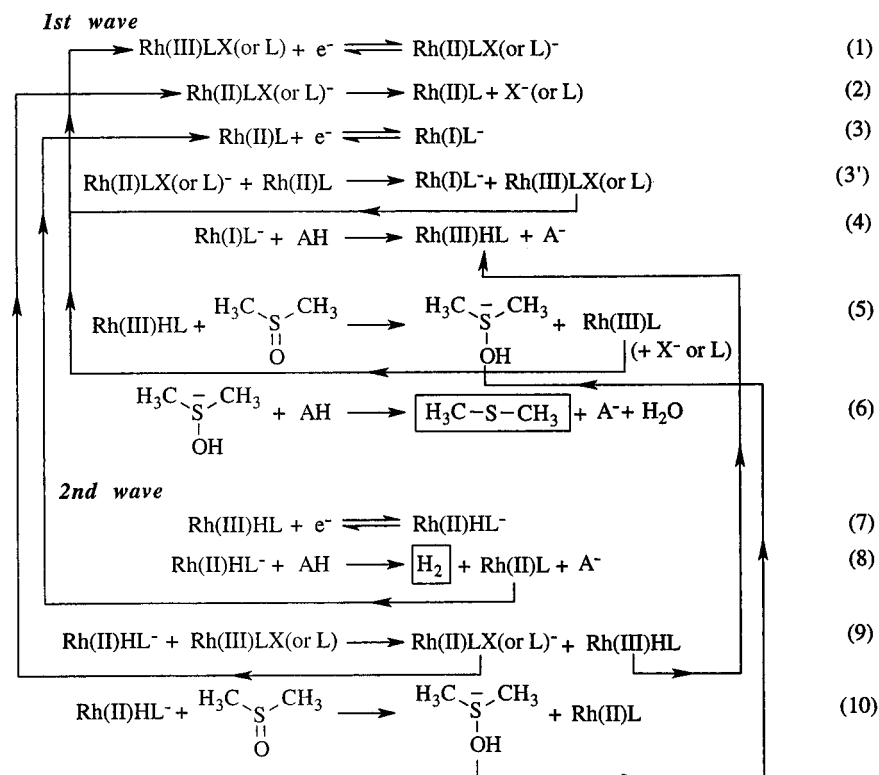


The results of the second electrolysis are summarized in Figure 4B. The porphyrin does not undergo a significant degradation during these electrolyses as checked by means of cyclic voltammety and UV-vis spectrometry.

The cyclic voltammety experiments shown in Figure 4A, as well as other experiments at other acid concentrations, indicate that, above a 5 mM concentration of CF<sub>3</sub>CO<sub>2</sub>H, the Rh(III)/Rh(I) wave becomes plateau-shaped, as expected for a catalytic wave with an excess substrate,<sup>6c</sup> with a height that remains constant upon further addition of the acid. Simultaneously, the Rh(III)H/Rh(II)H<sup>-</sup> wave increases and becomes higher than the first wave. We also note that the reoxidation wave of the Rh(I) complex disappears, indicating that it is involved in a fast protonation reaction followed by the rapid evolution of the Rh(III)H complex thus formed. All of these observations may be rationalized by the set of reactions depicted in Scheme 1.

At the first wave, the catalytic process starts with the two-electron reduction of Rh(III) into Rh(I) according to the ECE-disproportionation mechanism (steps 1-3'). The latter complex is then protonated (step 4) by the acid added and the ensuing rhodium(III) hydride reduces DMSO according to steps 5 and 6. At the potential of the second wave, the rhodium(III) hydride is first reduced into rhodium(II) hydride (step 7). With a relatively weak acid or with a small concentration of a strong acid, the rhodium(II) hydride is stable within the time scale of

## Scheme 1



the cyclic voltammetric experiment, which explains why the reversibility of the wave can be reached easily upon raising the scan rate (Figure 1c,d). When the strength and/or the concentration of the acid is increased, the rhodium(II) hydride reacts competitively with the acid (step 8) and with DMSO (step 10). In view of the respective location of the two standard potentials, it may also transfer an electron to the starting Rh(III) complex (step 9). Since reaction step 9 regenerates the rhodium(III) hydride, this opens a second pathway for the reduction of DMSO at the level of the second wave.

Thus, at low acid concentrations, or with a relatively weak acid, the catalytic process at the first wave is controlled by the rate of the reaction (step 4). This is the case until the rate of this reaction remains smaller than the reduction of DMSO (step 5). This condition is reverted upon increasing the acid concentration. Step 5 then becomes the rate-determining step, and consequently, the first wave catalytic current ceases to increase with the acid concentration. At the second wave, the catalytic current corresponding both to hydrogen evolution (step 8) and DMSO reduction (steps 9 + 10) continues to increase with the acid concentration because the production of the rhodium(III) hydride (step 4), and hence, the production of the rhodium(II) hydride (step 7) becomes faster and faster. Thus, the second catalytic wave increases faster than the first and becomes eventually higher. At low acid concentrations, on the order of the porphyrin concentration, the first catalytic wave is peak-shaped (Figure 4Aa), whereas it becomes plateau-shaped upon raising the acid concentration (Figure 4Ab,c). The latter situation implies that the catalytic process is fast as compared to diffusion and thus takes place within a thin reaction layer adjacent to the electrode.<sup>6c</sup> It also implies that the substrate, the acid in the present case, is in sufficient excess to be negligibly consumed within the reaction layer. When the acid concentration is so low that the latter condition is not fulfilled, the diffusion of the acid from the bulk of the solution to the electrode surface governs the catalytic current resulting in a peak-shaped wave ("total catalysis"<sup>6c</sup>).

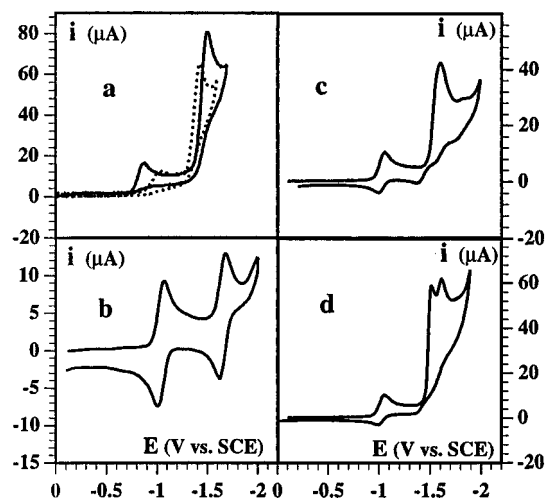


**Figure 5.** Effect of tertiary phosphines on the cyclic voltammetry of TPRhI (1 mM) in butyronitrile + 0.1 M *n*-Bu<sub>4</sub>NClO<sub>4</sub> in the presence of CNCH<sub>2</sub>CO<sub>2</sub>H: (a) 20 mM acid, dotted line no phosphine added, full line + 0.1 M PPh<sub>3</sub>; (b–d) +50 mM PEt<sub>3</sub>. Acid concn: 0 (b), 5 (c), 50 (d) mM. Scan rate: 0.1 V/s.

In butyronitrile also, catalysis is observed, but only at the level of the second (Rh(III)/Rh(II)) wave (Figure 5a). Electrolyses just beyond the peak of this wave were carried out in the presence of CNCH<sub>2</sub>CO<sub>2</sub>H and HCO<sub>2</sub>H. The results are summarized in Figure 6a. Strikingly, the faradaic yield for hydrogen evolution, as defined above, is, at the beginning of the electrolysis, much larger than 100%, reaching a value close to 200%. The decay of the faradaic yield and of the turnover number per hour with time parallels the degradation of the porphyrin as revealed by cyclic voltammetry and UV–vis spectrometry in the course of electrolysis. The red-orange solution becomes green. The initial bands at 422, 534, and 570 nm are replaced by bands at 418 and 532 nm and an intense band at 584 nm, pointing to the hydrogenation of the porphyrin

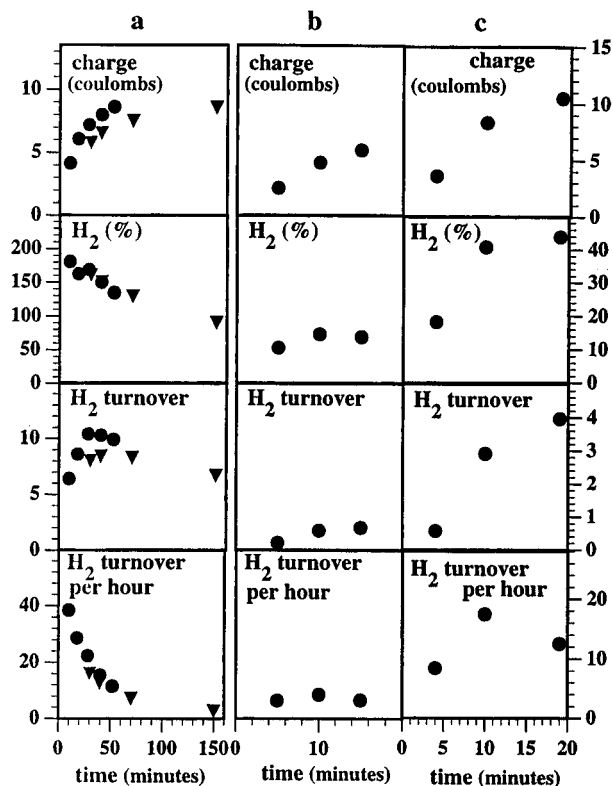
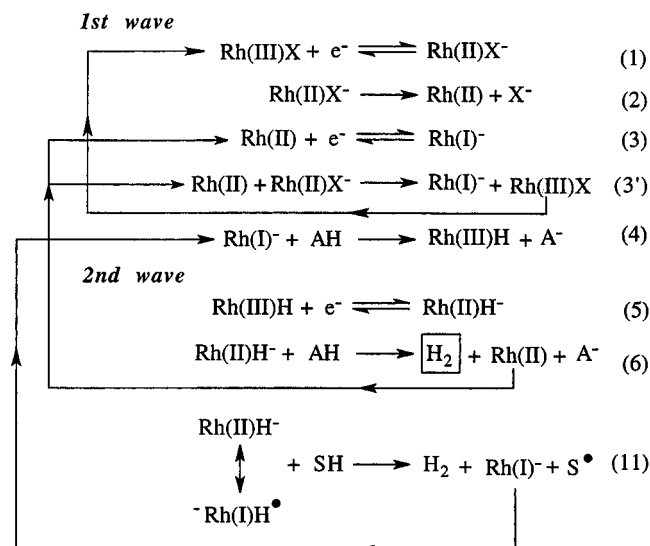


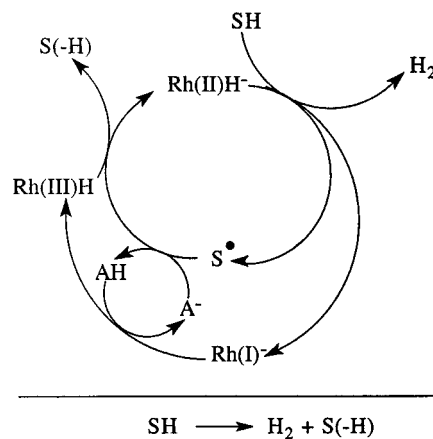
**Figure 6.** H<sub>2</sub> evolution from the preparative scale electrolysis at the Rh(III)H/Rh(II)H<sup>-</sup> wave of TPPRhI (1 mM) in butyronitrile + 0.1 M *n*-Bu<sub>4</sub>NClO<sub>4</sub> in the presence of acids: (a) 20 mM HCO<sub>2</sub>H (S), 20 mM CNCH<sub>2</sub>CO<sub>2</sub>H (J), no phosphine added; (b) 20 mM CNCH<sub>2</sub>CO<sub>2</sub>H + 0.1 M PPh<sub>3</sub>; (c) 20 mM CNCH<sub>2</sub>CO<sub>2</sub>H + 0.05 M PEt<sub>3</sub>.

### Scheme 2



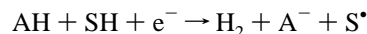
ring yielding a chlorine. These observations may be rationalized by the set of reactions represented in Scheme 2. At the first wave, the rhodium(I) porphyrin is still formed by the same two-electron ECE–disproportionation process (steps 1–3') as before and is converted into the rhodium(III) hydride by reaction with the acid (step 4). Unlike DMSO, butyronitrile is not reduced by Rh(III)H. Rh(II)H<sup>-</sup>, formed at the second wave (step 5), reacts with the acid, triggering the catalytic evolution of hydrogen (step 6) as in DMSO. However, the fact that the hydrogen faradaic yield exceeds 100% by a large amount indicates that the acid ceases to be the sole source of the evolving hydrogen. The only other possibility is hydrogen abstraction from any H-atom donor (noted SH in Scheme 2)

### Scheme 3

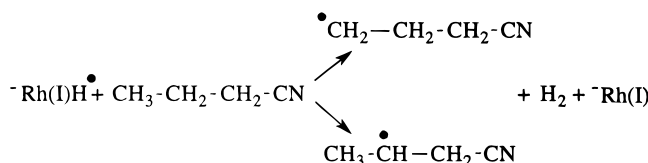


present in the solution (step 11). H-Atom abstraction by the Rh(II)H<sup>-</sup> complex implies that the contribution of the resonant rhodium(I) form shown in Scheme 2 is more important in butyronitrile than in DMSO. This difference between the two solvents falls in line with the fact that butyronitrile is certainly a poorer ligand of rhodium(II) than DMSO, thus increasing the contribution of the Rh(I) resonant form at the expense of the Rh(II) form in the rhodium(II) hydride. Less charge density on the hydrogen atom in butyronitrile may induce the presence of more charge density on the rhodium but also on the porphyrin ring, thus explaining why the catalyst decay is faster in butyronitrile than in DMSO.

H-Atom abstraction by the rhodium(II) hydride is accompanied by the cleavage of the Rh–H bond to form a molecule of hydrogen. The overall stoichiometry of H<sub>2</sub> production through H-atom abstraction is thus:



Keeping the same definition of the H<sub>2</sub> faradaic yield as before, its value would reach 200% if the reaction (step 11) were the predominant pathway for H<sub>2</sub> evolution. However, this is true only if the further reactions undergone by the radical S<sup>•</sup> do not involve an additional electron uptake at the electrode and/or in the solution. The solvent, butyronitrile, is a good candidate for H-atom abstraction and the solvent radicals thus formed may dimerize.



However, another possibility is that the latter radical gets deprotonated and reoxidized according to the reactions depicted in Scheme 3 where the dehydrogenated product, noted S(-H) in the scheme, stands for CH<sub>3</sub>CH=CHCN when H-atom transfer involves the solvent. Such a radical chain mechanism does not consume electrons. The electrode then merely serves as catalyst of the dehydrogenation reaction. Such electrochemically triggered radical chain processes are well-documented. They have been described in details in cases where the key step is H-atom scavenging by an aryl radical<sup>18</sup> and also when the key step is the addition of a nucleophile on an aryl radical leading to

(16) (a) Amatore, C.; Badoz-Lambling, J.; Bonnel-Hughes, C.; Pinson, J.; Savéant, J.-M.; Thiébaud, A. *J. Am. Chem. Soc.* **1982**, *104*, 1979. (b) Andrieux, C. P.; Badoz-Lambling, J.; Combellas, C.; Lacombe, D.; Savéant, J.-M.; Thiébaud, A.; Zann, D. *J. Am. Chem. Soc.* **1987**, *109*, 1518.

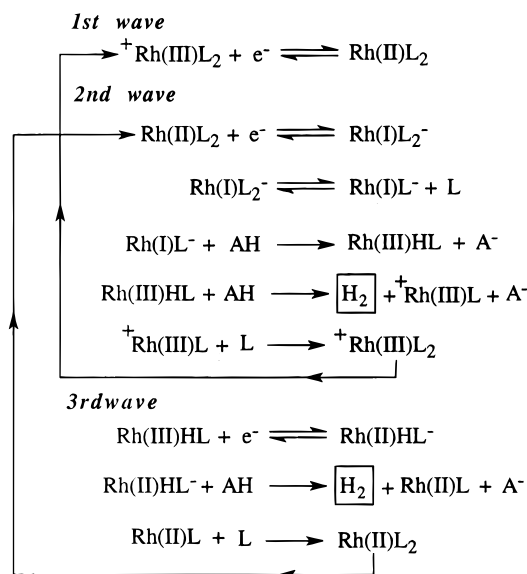
aromatic substitution of the  $S_{RN}1$  type.<sup>17</sup> The solvent may not be the sole source of H-atom. The tetralkylammonium cation of the supporting electrolyte may also play this role, in which case,  $SH = (n-C_4H_9)_4N^+$  and  $S(-H) = (n-C_4H_9)_3N + CH_2=CHCH_2CH_3$ . One or the other acid used may also act as H-atom donors. Then,  $SH = HCO_2H$ ,  $NCCH_2CO_2H$  and  $S(-H) = CO_2$ ,  $CO_2 + NCCH_2OH$ , respectively.

If the H-atom abstraction radical chain electrocatalytic mechanism is operating, a faradaic yield of 200% means that this process is in balanced competition with the hydride transfer pathway.

The comparison between the results obtained in butyronitrile and DMSO suggests that the presence of a second axial ligand in the rhodium(II) hydride is a governing factor in the competition between the hydride and H-atom transfer pathways. Triphenylphosphine may serve as such an axial ligand of the rhodium(II) hydride. In this connection, the significant negative shift of the  $Rh(II)H$  reduction peak observed upon addition of  $PPh_3$  to the butyronitrile solution (full line vs dotted line in Figure 5a) indicates that  $Rh(III)$  is more strongly complexed than  $Rh(II)H^-$  but does not dismiss the ligation of the latter by  $PPh_3$ . The height of this peak shows that an efficient catalysis process is taking place. The results of a preparative scale electrolysis in the presence of  $PPh_3$  are displayed in Figure 6b. The value of the faradaic yield, ca. 20%, indicates that the hydride pathway predominates, thus confirming the role of axial ligand in the hydride/H-atom transfer dichotomy. There is a rapid degradation of the porphyrin ring, as revealed by cyclic voltammetric and spectrophotometric assays during the course of the electrolysis. This may be due to a distribution of the charge density in the rhodium(II) hydride that would be more in favor of localization on the porphyrin ring than with DMSO. Degradation may also occur at the level of the rhodium(I) in competition with the bonding of  $H^+$  with the rhodium atom (step 4 in Scheme 2).

While  $PPh_3$  does not alter the ECE-disproportionation two-electron conversion of rhodium(III) in to rhodium(I), other tertiary phosphines, such as triethylphosphine, completely change the reduction mechanism.<sup>11</sup> The rhodium(I) complex is then formed following two well-separated reversible one-electron transfer reactions, as recalled in Figure 5b. Upon addition of an acid, the rhodium(II)/rhodium(I) wave becomes catalytic while the rhodium(III)/rhodium(II) wave remains unchanged (Figure 5c,d). This means that catalysis is triggered by the formation of the rhodium(III) hydride formed upon protonation of the rhodium(I) complex. At a low acid concentration, a small wave appears beyond the second (catalytic) which may be ascribed to the reduction of the rhodium(III) hydride produced at the preceding wave (Figure 5c). Catalysis at the second wave is then so efficient that all of the acid is consumed at the electrode surface (total catalysis), which prevents the third wave from becoming catalytic. However, the third wave becomes eventually catalytic upon raising the acid concentration (Figure 5d). The results of an electrolysis performed in the potential region of the catalytic waves are displayed in Figure 6c. The faradaic yield for hydrogen evolution reaches 40%, and degradation of the porphyrin ring during electrolysis is still observed. These observations may be rationalized by the set of reactions represented in Scheme 4. The introduction of triethylphosphine as axial ligand induces a striking change in the mechanism of hydrogen evolution, namely

#### Scheme 4



the rhodium(III) hydride is now catalytically active, whereas only the rhodium(II) hydride was active in the preceding cases. This increased reactivity of the rhodium(III) hydride toward the acid is likely to be caused by the increased electron density on the hydrogen atom bound to rhodium caused by the presence of a strong electron donor such as  $PEt_3$  in the rhodium coordination sphere.

#### Conclusions

Rhodium(III) porphyrins are reduced directly into rhodium(I) complexes in polar solvents according to a two-electron ECE-disproportionation process. Electrogenerated rhodium(I) porphyrins react readily with acids affording the rhodium(III) hydrides which give rise to the rhodium(II) hydrides at a more negative potential. The latter reaction is reversible at low acid concentrations but the rhodium(II) hydride catalyzes hydrogen evolution as the concentration and/or its strength increase. DMSO is catalytically reduced by both the rhodium(III) and the rhodium(II) hydride. The latter reactions thus compete with the rhodium(II) hydride catalysis of hydrogen evolution. A striking change of mechanism occurs when a poorly ligating solvent such as butyronitrile is used. Faradaic yields of hydrogen evolution larger than 100% are thus obtained indicating that H-atom abstraction from the solvent, or from other H-atom donors present in the solution, competes with the hydride transfer reactivity of the rhodium(II) hydride. The H-atom transfer reactivity of the rhodium(II) hydride is suppressed by addition of strong and soft ligands such as tertiary phosphines. When triphenylphosphine is added to a butyronitrile solution, the rhodium(I) complex is still produced directly from the two-electron reduction of the rhodium(III) porphyrin. The main role of the phosphine is then to serve as an axial ligand to the rhodium(II) hydride, thus increasing its hydride transfer reactivity at the expense of its H-atom transfer reactivity. More electron-donating phosphines, such as triethylphosphine, have an even more pronounced effect on the electrochemistry of rhodium porphyrins and on their ability to catalyze hydrogen evolution. The rhodium(I) complex is then formed after two well-separated reversible one-electron uptakes. Protonation then leads to the rhodium(III) hydride which is able to catalyze hydrogen evolution, unlike what occurs in the other cases. The rhodium(II) hydride still remains able to catalyze hydrogen evolution following its formation at a more negative potential.

(17) (a) Savéant, J.-M. *Acc. Chem. Res.* **1980**, *13*, 323. (b) Savéant, J.-M. *Adv. Phys. Org. Chem.* **1990**, *26*, 1. (c) Savéant, J.-M. *Tetrahedron* **1994**, *50*, 10117.

(18) (a) Gueutin Claire, Thèse de l'Université Denis Diderot, Paris, 1991. El Kasmi, A. Thèse de l'Université Denis Diderot, Paris, 1991.

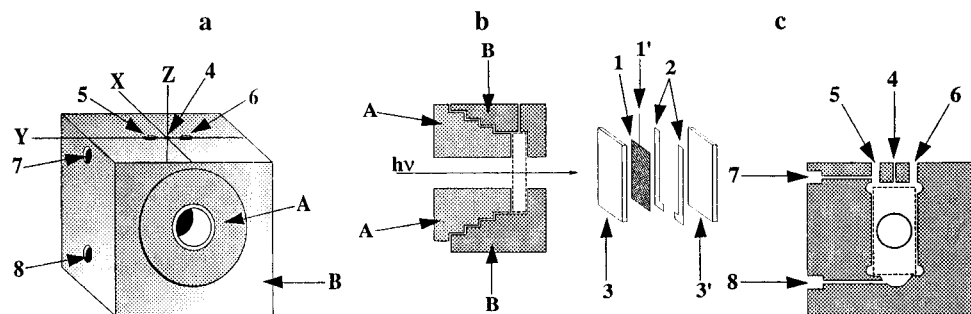


**Figure 7.** IR spectroelectrochemistry cell: (a) general view; (b) XZ view; (c) YZ view.

These changes in reactivity produced by the variation of axial ligands can be rationalized in terms of the electron density distributions they induce at the level of the rhodium and bound hydrogen atoms. The variations of the stability of the catalyst with the nature of the axial ligand are likewise explainable by changes in the electron density distribution at the level of the porphyrin ring.

### Experimental Section

The various chemicals used in this work were from the same origin as in ref 11. The cells and instrumentation for cyclic voltammetry and thin-layer spectroelectrochemistry were the same as previously described.<sup>11</sup> The cell for preparative scale electrolysis was modified to allow for the analysis of hydrogen evolution (Figure 7). All electrolyses were carried out in a water- and oxygen-free glovebox. The production of hydrogen in the gas phase was determined by gas

chromatography (Delsi instrument with a catharometric detector and 4 m silica gel column).

The cell used for IR spectroelectrochemistry was as depicted in Figure 7.<sup>18</sup>

The cell is made of two assembled Teflon blocks, A and B. A 0.3 mm thick platinum grid (1) serves as the working electrode. It is connected to the potentiostat by 1' through entry 4. The working electrode is sandwiched between two  $\text{CaF}_2$  windows (3 and 3'), separated by the spacer 2. The counterelectrode (a Pt wire) and the reference electrode ( $\text{Ag } 0.01 \text{ M AgClO}_4$ ) are protected by salt bridges containing the supporting electrolyte solution and penetrate in the cell by entries 5 and 6, respectively. After the electrodes are introduced, the air in the gap cell is flushed out by argon through 7 and 8, the cell is filled, and 7 and 8 are sealed with septa.

JA964100+